Available online at www.sciencedirect.com
ScienceDirect
Trans. Nonferrous Met. Soc. China 29(2019) 849−858
Transactions of Nonferrous Metals Society of China
www.tnmsc.cn

Improving vanadium extraction from stone coal via combination of blank roasting and bioleaching by ARTP-mutated *Bacillus mucilaginosus*

Ying-bo DONG[1,2], Yue LIU[1], Hai LIN[1,2], Chen-jing LIU[1]

1. School of Energy and Environmental Engineering,
University of Science and Technology Beijing, Beijing 100083, China;
2. Beijing Key Laboratory on Resource-oriented Treatment of Industrial Pollutants, Beijing 100083, China

Received 7 May 2018; accepted 24 July 2018

Abstract: In order to improve leaching efficiency of vanadium from stone coal, the combination of blank roasting and bioleaching using *Bacillus mucilaginosus* (*B. mucilaginosus*) mutants was evaluated. The atmospheric and room temperature plasma (ARTP) technique was used to generate *B. mucilaginosus* mutants. The results showed that a mutant *B. mucilaginosus* BM-50, after ARTP irradiation for 50 s, had the highest acid production. The total content of the organic acid produced by *B. mucilaginosus* BM-50 was nearly doubled compared with the wild strain after 2 days. After 20 days, vanadium leaching rate with *B. mucilaginosus* BM-50 reached 18.2%, which was improved compared with the original bacteria (15.3%). A pretreatment via blank roasting for stone coal further improved the vanadium dissolution by bioleaching, namely, 68.3% vanadium was extracted, which was much higher than that without blank roasting. It is shown that bioleaching by bacterial mutants by ARTP irradiation combined with blank roasting has great potential for improving vanadium recovery from low-grade vanadium bearing stone coal.

Key words: atmospheric and room temperature plasma (ARTP); *Bacillus mucilaginosus*; vanadium-bearing stone coal; blank roasting; bioleaching

1 Introduction

Vanadium (V) is an important rare element and is extensively used in many fields, including the steel industry, titanium−aluminum alloys, vanadium redox battery and catalysts [1]. Stone coal is recognized as a specific vanadium-bearing resource in China. The gross reserve of vanadium (V_2O_5) in stone coal is 118 million tons, which accounts for over 87% of the domestic reserve of vanadium [2]. Various vanadium extraction techniques for stone coal have been investigated, like roasting, acid leaching, ion purification, precipitation, and calcination [3]. Extracting vanadium from stone coal is commonly confronted with the issues of the enormous ore handling quantity, the high acid consumption, and the high production cost [4]. In order to solve these problems, bioleaching is considered as one of the strategic and perfect processing technologies for utilizing mineral resources, where extensive studies have been conducted to extend its application within metallic minerals.

There are some significant advantages associated with bioleaching, such as low investment and energy consumption, with the benefits to the environment [5]. In the past several decades, bioleaching has been successfully applied in metallurgical industries, such as copper, uranium, gold, and cobalt extractions [6,7]. There is less research regarding extracting V in vanadium-bearing stone coal using microbial leaching technology. Previous studies primarily used *Thiobacillus*, which demonstrated a lower leaching rate [8]. The low leaching rate could be due to the fact that most vanadium within stone coal exists in the crystal lattice of the aluminosilicate minerals and isomorphically replaces Al(III) in muscovite [9], where the *Thiobacillus* cannot destroy the lattice structure.

Previous studies have shown that silicate bacteria could influence the decomposition and transformation of silicate minerals [10]. For example, after a 20-day interaction with *B. mucilaginosus* D4B1, the expansion ratios of montmorillonite samples decreased from 83.2% to 76.7% [11]. The actions of quartz and indigenous

Foundation item: Project (2015ZX07205003) supported by Major Science and Technology Program for Water Pollution Control and Treatment of China
Corresponding author: Hai LIN; Tel: +86-10-62333603; E-mail: linhai@ces.ustb.edu.cn
DOI: 10.1016/S1003-6326(19)64995-2

Bacillus spp. have been tested by STYRIAKOVA et al [12], which showed that the bacteria assisted the release of Fe via the dissolution of quartz particles. *B. mucilaginosus*, known as a silicate bacterium, is often used as a model strain for studying the role that bacteria play in the weathering processes of silicates [13].

ARTP is a powerful physical microbial mutagenesis tool used for microorganism breeding. The ARTP mutation system has been successfully applied for mutating *S. platensis*, which enables the generation of mutant 3-A10 with 40.3% higher carbohydrate productivity than the wild-type strain [14]. LI et al [15] also applied ARTP to the mutagenesis of the oleaginous fungus, *Mortierella Alpina*. The results showed that the arachidonic acid production of mutant strain D20 (5.09 g/L) was increased by 40.61%, more than the original strain (3.62 g/L).

Previous studies showed that the application of different enhanced treatments, such as supplement of sucrose, adding surfactant, and roasting pretreatment, improved the metals recovery in the bioleaching process [16]. Research by LIU et al [17] showed that the cobalt leaching efficiency could be boosted by more than 21% when 0.1 g/L of surfactant (Tween-20) was added. ZHAO et al [18] found that vanadium was liberated from the crystal structure of mica through roasting, which improved the recovery of vanadium.

Bioleaching technology was chosen to recover vanadium from stone coal in this study. *B. mucilaginosus* was selected as the experimental bacterium because it could destroy the silicate mineral structure. ARTP mutagenesis and various enhanced treatments were used to improve the V leaching and to achieve the reutilization of V from a low-grade vanadium-bearing stone coal.

2 Experimental

2.1 Microorganisms and culture media

The *Bacillus mucilaginosus* (the CGMCC number: 1.0910) was purchased from China General Microbiological Culture Collection Center (CGMCC). The bacterium was aerobically cultured in a silicate bacterial culture medium, which comprised of sucrose (5 g/L), $Na_2HPO_4·12H_2O$ (3.0 g/L), $CaCO_3$ (0.1 g/L), $(NH_4)_2SO_4$ (2 g/L), $MgSO_4$ (0.5 g/L), KCl (0.1 g/L) and $FeCl_3$ (0.005 g/L). The composition of the agar medium was silicate bacterial culture medium and agar (15 g/L). The initial pH was adjusted to 7.0 with 10% H_2SO_4. The bacteria were cultured in flasks which were shaken in an air thermostat shaker at 180 r/min and 30 °C.

2.2 Mineral samples

The vanadium-bearing stone coal was sourced from Yunxi, Hubei province, China. The samples were prepared by crushing and screening the material to particle sizes below 74 μm. The particles were analyzed for their chemical contents via X-ray fluorescence (XRF). The chemical composition of the stone coal is given in Table 1. The main component of the stone coal was SiO_2. The V_2O_5 content was 1.19%. X-ray diffraction (XRD) analysis with the scanning rate of 6 (°)/min from 10° to 100° was used to detect mineral phases. The X-ray diffraction pattern (Fig. 1) showed that the main mineral phase was quartz, followed by muscovite.

Table 1 Chemical composition of vanadium-bearing stone coal (wt.%)

SiO_2	BaO	Fe_2O_3	Al_2O_3	SO_3	CaO	V_2O_5	MgO
76.45	4.49	3.87	3.71	3.25	2.80	1.19	1.17
K_2O	P_2O_5	ZnO	Cr_2O_3	CuO	TiO_2	I	
1.07	0.63	0.46	0.21	0.19	019	0.07	
MnO	NiO	Na_2O	PbO	Cl	SnO_2	SeO_2	
0.06	0.05	0.05	0.05	0.03	0.02	0.01	

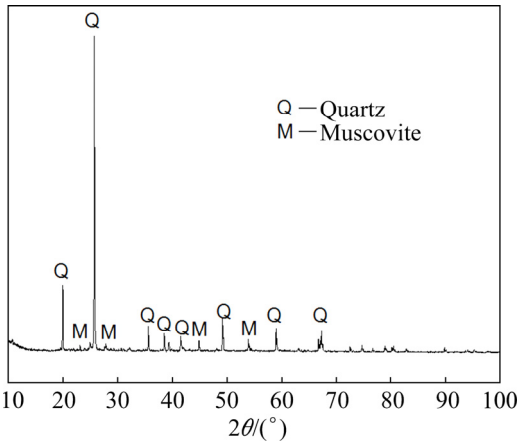

Fig. 1 XRD pattern of stone coal

2.3 ARTP mutagenic treatment

The ARTP mutation breeding system used in the experiment was a multifunctional plasma mutagenesis instrument (MANDELA, Beijing Wei Nesi Technology Co., Ltd., China). ARTP mutation was performed when *B. mucilaginosus* cell growth was in the logarithmic phase, with a cell density of 10^4−10^5 CFU. Pure helium was used as the plasma working gas during the ARTP mutation. The operating parameters were as follows: (1) the gas flow was 10 L/min, (2) the distance between the plasma torch nozzle exit and the sample plate was 2 mm, and (3) the temperature of the plasma jet was 23.0−35.0 °C. At first, 20 μL of fresh bacterium suspension was uniformly coated on the sterilized steel plates. Then, they were exposed to the ARTP jet for 10, 20, 30, 40, 50, 60, 70, 80 and 90 s, respectively. An exposure for 0 s was used as the control (wild strain).

After each treatment, 980 μL of sterile water was added to the steel plate for dilution. 100 μL of diluted solution was used to coat the agar medium for 48 h at 30 °C. The lethality rate was determined by counting the individual colonies formed by wild strain and each mutant.

2.4 Bioleaching tests

All bioleaching tests were performed in 250 mL Erlenmeyer flasks with 100 mL of sterilized culture medium. The initial pH was adjusted to 7.0 with 10% H_2SO_4. The 1% (vol.%) original bacteria or the mutagenic bacteria in a logarithmic phase were added to each flask. The pulp density was 1% (wt.%). All flasks were shaken in an air thermostat shaker at 180 r/min and 30 °C. During the experiments, leachate was periodically collected from each flask to determine the pH and the heavy metals concentrations.

2.5 Enhanced treatments

To further improve the vanadium removal after ARTP mutagenesis, three types of enhanced treatments were selected: supplement of sucrose, adding surfactant, and roasting. The leaching system without any enhanced treatments was set as the blank control.

(1) Supplement of sucrose

Two methods were set to supplement the carbon source. Plan A: adding 5 g/L of sucrose to the flask every four days during the bacterial leaching process. Plan B: increasing initial concentrations of sucrose from 5 to 25 g/L.

(2) Adding surfactant

Two types of surfactants were selected to add to the bioleaching system in accordance with the classification of surfactants: Tween-20 and sodium dodecyl sulfate (SDS). The concentration of the surfactants were 0.05, 0.1 and 0.2 g/L.

(3) Roasting

Stone coal samples were placed in a porcelain dish to roast without any additives as a pretreatment.

2.6 Analysis methods

The growth curve of each mutant was measured via a Bioscreen automatic growth curve analyzer. The concentrations of Si, Al, and V in the leachate and the pH values were measured using an inductively coupled plasma emission spectrometer (ICP-OES) and an S20seveneasy pH meter, respectively. The content of organic acid in the medium solution was determined by an LC−2030 high-performance liquid chromatography (HPLC), manufactured by Japan Shimadzu Corporation. The surface morphology changes of the stone coal before and after leaching were explored with scanning electron microscopy (SEM) equipped with energy-dispersive microanalysis facilities (EDS). Fourier transform infrared (FTIR) spectra in the mid-IR (MIR) region (4000−400 cm^{-1}) were obtained by using a Nicolet Nexus 670 FT-IR spectrometer.

2.7 Statistical analysis

All experiments were performed in triplicate. Analysis of means and standard deviations were done by using Microsoft Excel Software, version 2016.

3 Results and discussion

3.1 Effect of ARTP

In this study, the ARTP dose applied to the bacterial sample was dependent on treatment time. The effect of various treatment time on the lethality rates of *Bacillus mucilaginosus* is shown in Fig. 2.

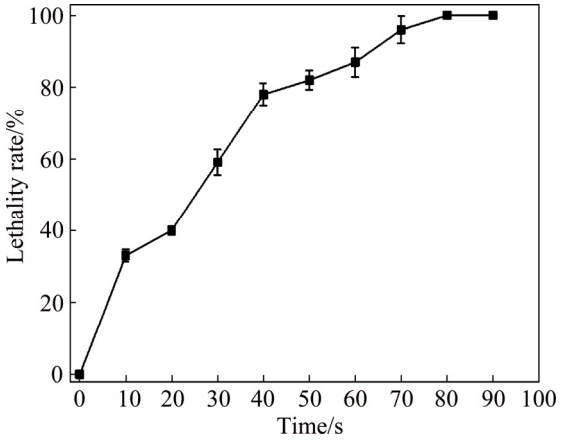

Fig. 2 Effect of treatment time on lethality rates of *Bacillus mucilaginosus*

Figure 2 shows that when the treatment time was 50, 60 and 70 s, the lethality rates reached 82%, 87%, and 96%, respectively. When the mutation treatment time was over 80 s, all bacteria were killed. It was found in previous studies that exposure time and lethality rate is proportional to a certain range, where longer exposure time led to higher lethality, which affected the mutation rate [19]. During the mutation process, the particles produced by ARTP could alter the physicochemical properties of the cell wall and the cell membrane, causing tissue damage. The cells were forced to start the SOS repair mechanism with high fault tolerance level, which produced a variety of the mismatch sites in the repair process. This finally allowed the genetic stability of the mutant strains [20]. The modern theory of breeding states that: when the mortality rate of microorganism mutagenesis reached 80%−90%, the positive mutation rate was the highest and the mutation effect was considered optimum [21].

The growth curves of *B. mucilaginosus* and mutagenic bacteria are shown in Fig. 3. The growth rate

of *B. mucilaginosus* rapidly increased from 4 to 16 h, which was obviously in the logarithmic phase. The growth rates during 16−20 h were relatively stable, and the growth rates started to decrease at 20 h. Figure 4 presents the pH curve of the *B. mucilaginosus* and the mutagenic bacterial strains. The pH value in the solutions decreased from 7 to 4 during the initial 12 h, likely because of the acidic metabolites produced by the bacteria [22]. The pH stabilized at <4. The pH of the mutant ARTP with a treatment time of 50 s (*B. mucilaginosus* BM-50) dropped rapidly and stabilized at 3.58, which was lower than that of the original bacterial culture (pH 4.00). The results inferred that the growth curves of all mutants were better than those of the original strain, but the difference was not significant, and the *B. mucilaginosus* BM-50 showed the best acid- production performance.

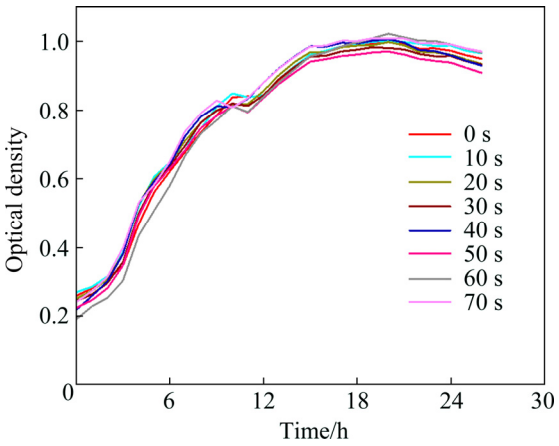

Fig. 3 Growth curves of *Bacillus mucilaginosus* and mutagenic bacteria

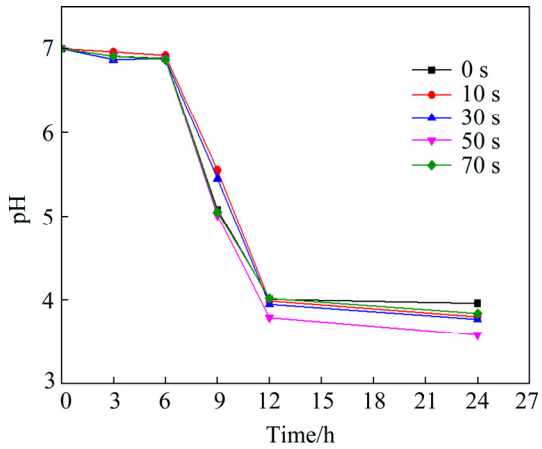

Fig. 4 pH curves of *Bacillus mucilaginosus* and mutagenic bacteria

The results of the HPLC showed that oxalic acid, tartaric acid, citric acid and malic acid were detected in the fermentation broth of both the original strain and the *B. mucilaginosus* BM-50 during cultivation (Fig. 5). Previous studies have reported that *Bacillus mucilaginosus* produces organic acid, and this could be the cause for the decreased pH value in the culture medium [23]. YANG et al [11] studied the effect of *B. mucilaginosus* D4B1 on the montmorillonite structure. The results suggested that the alteration in the mineral structure of montmorillonite could be triggered by the organic acids produced by bacteria. The content of organic acid increased with the incubation time, during the initial phase (1−2 days). As time progressed, the organic acid content (except tartaric acid) declined. The results indicated that when the bacteria grew and were reproduced, the organic acids that the cell synthesized and secreted into the fermentation broth were used as nutrients by bacteria. This is caused by the continuous depletion of nutrients in the medium. This finding agrees with the previous report. XIAO et al [24] found that the decrease of organic acids in solution was due to the use of silicate bacteria as nutrients when nutrients were scarce. The yield of the organic acids in the fermentation broth of *B. mucilaginosus* BM-50 was greater than that in the original bacterium. The total content of the organic acid produced by the original strain was 82.6 mg/L on day 2, while that of the *B. mucilaginosus* BM-50 was 162.6 mg/L.

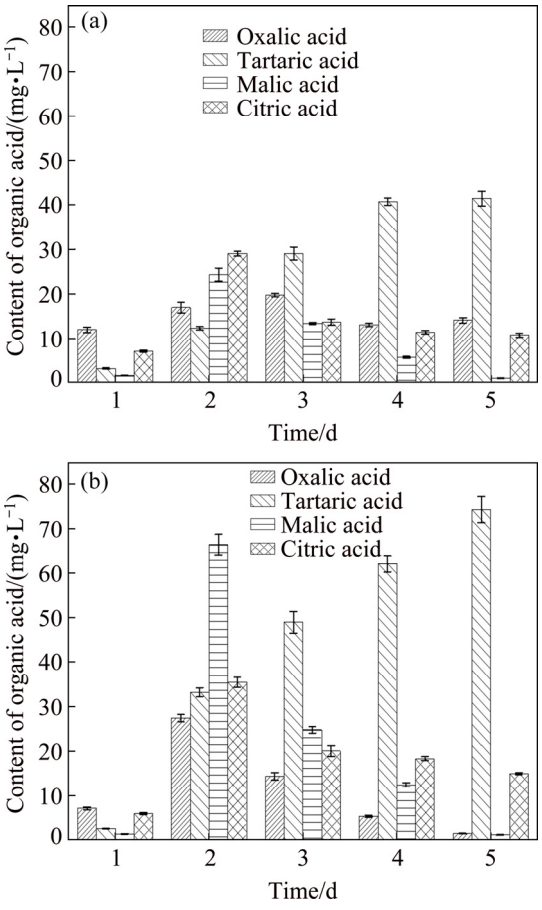

Fig. 5 Organic acid content of original bacteria (a) and *B. mucilaginosus* BM-50 (b) with different incubation time

3.2 Bioleaching effect of ARTP mutants

The pH curves and leaching efficiency of the vanadium-containing stone coal by *B. mucilaginosus* are shown in Fig. 6. The pH values of all cultures showed a similar trend (Fig. 6(a)), which initially decreased and then increased. The mutants showed different extents of change during the various treatment time. The *B. mucilaginosus* BM-50 showed a large decline. The pH dropped during the initial period, due to the organic acid that was produced by the bacterial metabolism. As the bioleaching time increased, the pH value increased. This indicated that the medium had poor nutrition, which caused the bacteria to use the organic acids and the extracellular polysaccharide as nutrients. Figure 6(b) shows that the V leaching rates of all strains were similar, and the highest leaching rate of *B. mucilaginosus* BM-50 was 18.2%, while that of original bacterial was 15.3%.

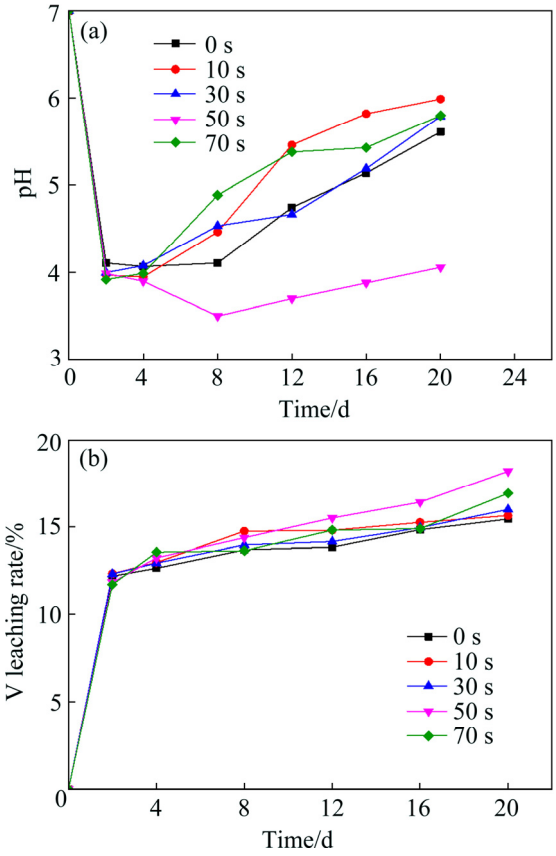

Fig. 6 pH curves (a) and V leaching rates (b) via original bacteria and mutant bacteria

3.3 SEM−EDS analysis of vanadium-bearing stone coal

3.3.1 Morphological changes of mineral surface

The SEM−EDS images of the raw stone coal and the bioleaching residue are shown in Fig. 7. The flat and undamaged mineral surface of the raw samples is shown in Fig. 7(a). The samples shown in Fig. 7(b) that reacted with bacteria were fragmentary and contained etch pits and had fuzzier surfaces than the raw samples. The leaching residues of the mutagenesis bacteria (Fig. 7(c)) showed more etch pits than the original bacteria, and the surface attachments were thicker and closer. The EDS results showed that the Si, Al and V contents in the residue decreased compared to the raw coal, and the reduction of the element contents in the residue after acting with *B. mucilaginosus* BM-50 was more significant. It was found in previous literature that during leaching, the bacteria attached to the surface of the mineral particles and their metabolites, such as organic acid and polysaccharides, were used to acidify and chelate the mineral particles. This damaged the weak chemical bonds of the particles and released metal elements [25].

3.3.2 Element distribution analysis on mineral surface

The element distributions on the raw stone coal surface and the bioleaching residue are shown in Figs. 8−10. The area fractions of the elements O, Si, O and Al on the samples (Fig. 9) that reacted with the bacteria were less than those of the raw material (Fig. 8). The decrease extent of these elements shown in Fig. 10 was more obvious. The results showed that SiO_2, V and Al gradually dissolved, due to the interactions between bacteria and their metabolites with mineral particles, where the mutagenesis bacteria played a significant role.

3.4 FTIR analysis of vanadium-bearing stone coal

Infrared spectroscopy was used to examine the possible changes in the minerals after bioleaching. Figure 11 depicts the FTIR spectra of the raw stone coal and the treated stone coal after bioleaching. Previous literature [26] stated that the peak at 3423 cm^{-1} was attributed to the H—O—H stretching vibrations of the water molecules between mica layers. The peaks at 1596 and 1625 cm^{-1} were attributed to the OH^- bending vibrations. The band at 1440 cm^{-1} was attributed to the CO_3^{2-} vibrations of carbonate minerals. The peak at 1080 cm^{-1} was attributed to the Si—O—Si asymmetric stretching vibrations. The peaks at 790 and 690 cm^{-1} were attributed to the Si—O—Si symmetrical stretching vibrations. The remaining peaks at 516 and 470 cm^{-1} were attributed to the Si—O—M bending vibrations.

The infrared spectra of minerals changed after bioleaching. First of all, the peak at 3409 cm^{-1} shifted to the higher wavenumber of 3453 cm^{-1} and a new peak appeared in bioleaching residue of original bacteria at 1623 cm^{-1}. That is, the hydrogen bonds in the interlayer water have changed, which meant that the cations in the mica structure changed [27]. The vibration peak of CO_3^{2-} at 1440 cm^{-1} in raw stone coal disappeared, which meant that small amounts of carbonate minerals in the raw mineral were decomposed after bioleaching. The

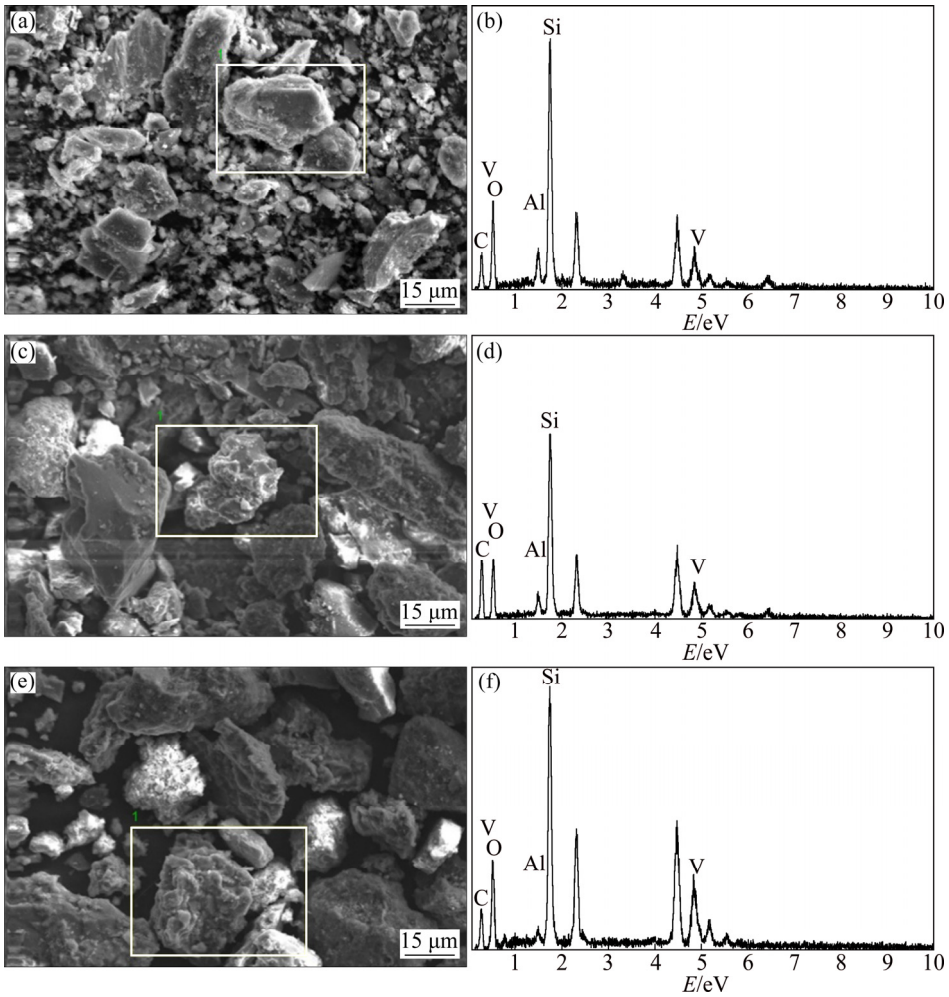

Fig. 7 SEM images (a, c, e) and EDS analysis results (b, d, f) of raw stone coal and bioleaching residue: (a, b) Raw stone coal; (c, d) Bioleaching residue of original bacteria; (e, f) Bioleaching residue of *B. mucilaginosus* BM-50

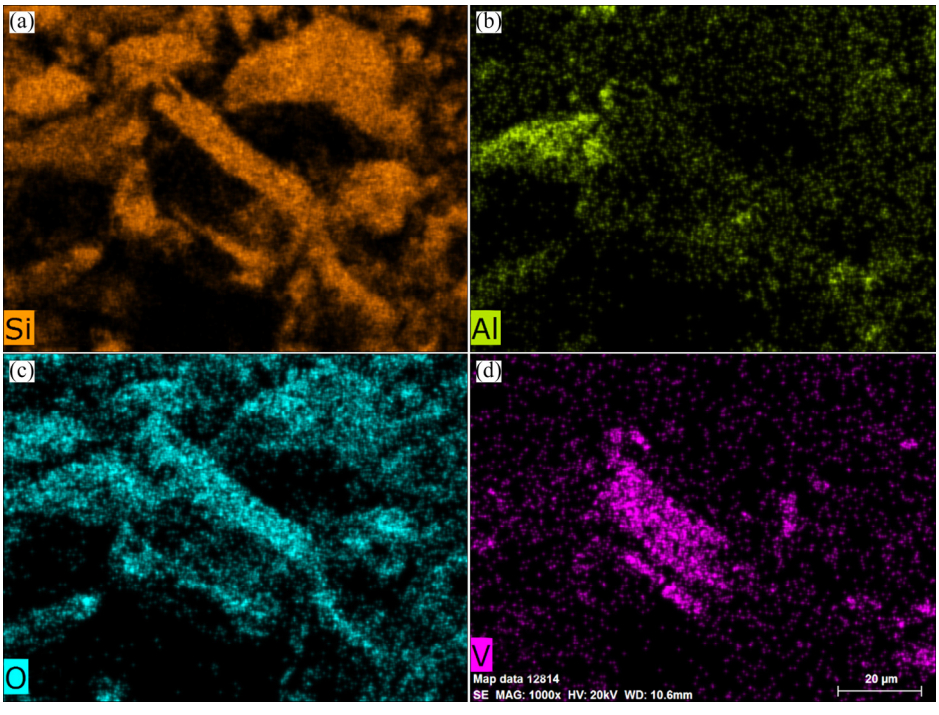

Fig. 8 Element distributions on raw stone coal surface: (a) Si; (b) Al; (c) O; (d) V

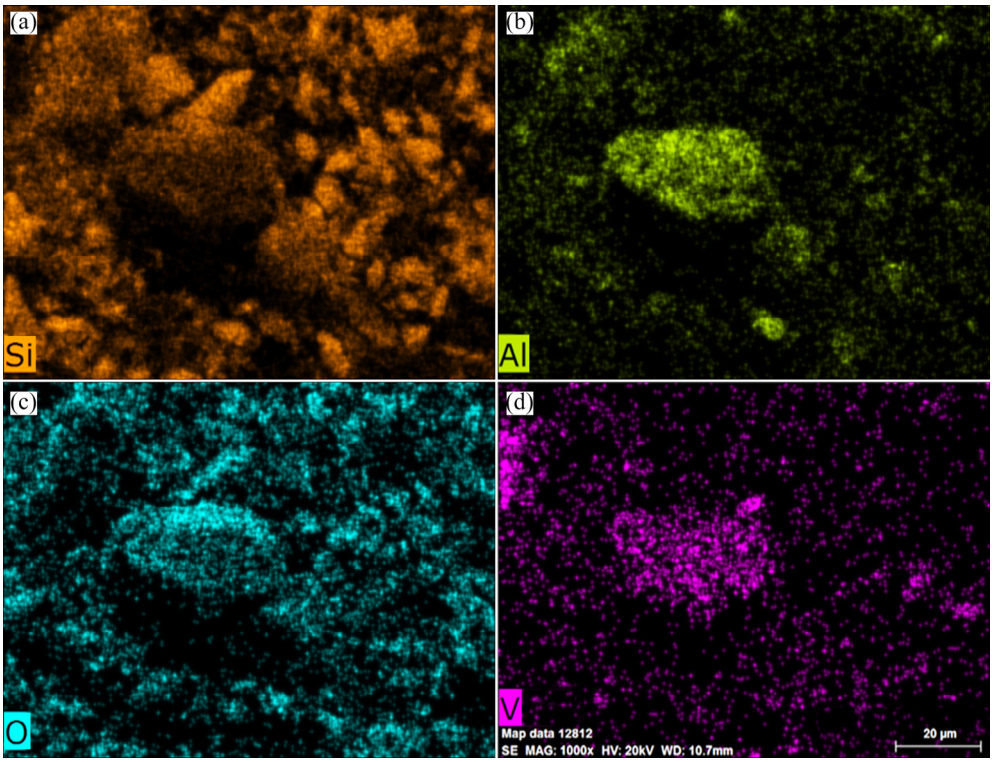

Fig. 9 Element distributions on bioleaching residue of original bacteria: (a) Si; (b) Al; (c) O; (d) V

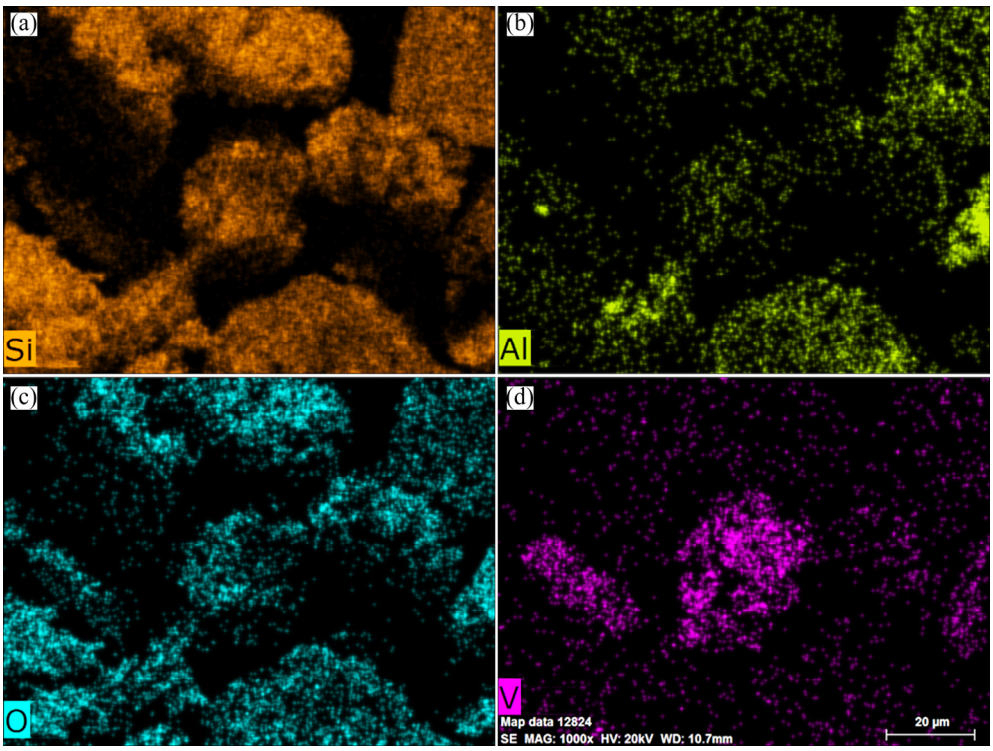

Fig. 10 Element distributions on bioleaching residue of *B. mucilaginosus* BM-50: (a) Si; (b) Al; (c) O; (d) V

peak of Si—O—Si asymmetric stretching vibrations at 1080 cm^{-1} was weakened obviously, which indicated that symmetry of the chemical bonds in the lattice became worse. The disappearance of the peak of Si—O—M bending vibrations at 516 cm^{-1} might be caused by the dissolution of metal ions, which indicated that the basic elements of mica in the stone coal were distorted and collapsed after leaching by bacteria and their metabolites [28]. The intensity of the band of residue leached by *B. mucilaginosus* BM-50 was stronger than that by original bacteria, which meant that mutagenic strain played a greater role in bioleaching on stone coal.

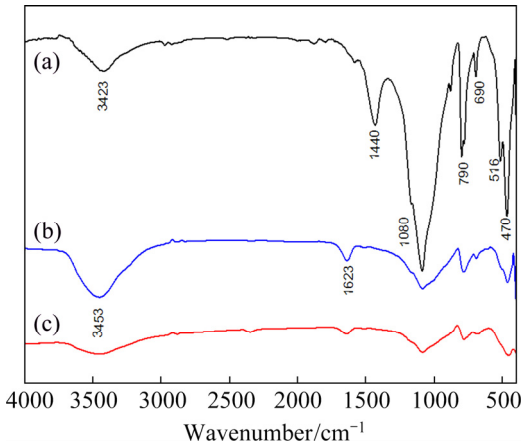

Fig. 11 FTIR spectra of raw stone coal and bioleaching residue stone coal: (a) Raw stone coal; (b) Bioleaching residue of *B. mucilaginosus* BM-50; (c) Bioleaching residue of original bacteria

3.5 Effect of enhanced treatments on bioleaching rate of vanadium

The vanadium removal performance and the organic acid production of *Bacillus mucilaginosus* were improved after ARTP mutagenesis. Various enhanced treatments were selected to further improve the effects of V extraction, where BM-50 was chosen as the experimental bacteria that demonstrated a better bioleaching effect.

3.5.1 Supplement of sucrose

The result of bioleaching by strain *B. mucilaginosus* BM-50 with the supplementing sucrose is shown in Fig. 12. As shown in Fig. 12(a), the leaching rate of the vanadium gradually increased when sucrose was added for 4 days. The leaching rate was 24.0% after 20 days of leaching, while that without supplementation was 18.2%. The V leaching rate increased slowly during the initial stage when the supplement was added, which rose rapidly during the late stage reaching 26.4% after 20 days after leaching. The pH curve (Fig. 12(b)) of the system with added supplementation showed that the pH remained stable and did not rebound after it dropped, which indicated that the energy source in the leaching system was sufficient and the metabolites produced by the bacteria were not consumed.

3.5.2 Adding surfactant

As shown in Fig. 13, the leaching rate initially increased and then decreased as the Tween-20 dosage increased. When the Tween-20 dosage was 0.05, 0.1 and 0.2 g/L, the V leaching rate reached 20.5%, 28.9% and 28.3%, respectively, after 20 days of leaching. The leaching rate gradually decreased as the dosage of SDS increased. When the SDS dosage was 0.05, 0.1 and 0.2 g/L, the leaching rate reached 30.1%, 26.2%, and 21.7%, respectively, after 20 days of leaching. The V

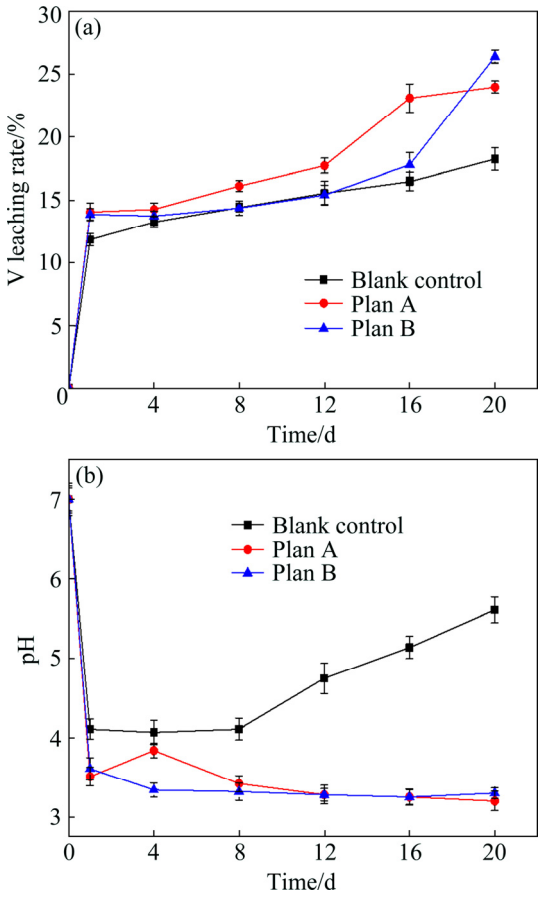

Fig. 12 V leaching rate (a) and pH curve (b) of bioleaching system with various supplementation methods

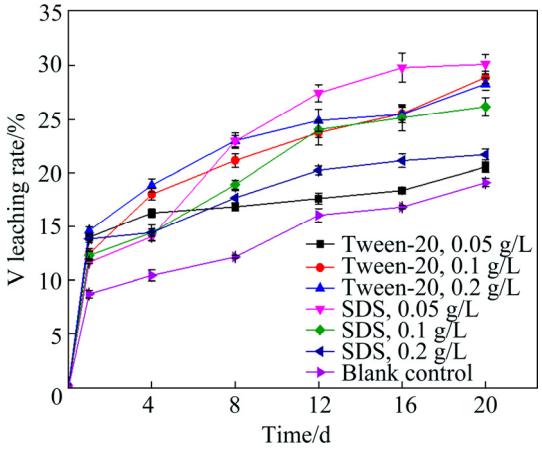

Fig. 13 V leaching rate of bioleaching system with various surfactants

leaching rate of the system without a surfactant was 19.1%. The results showed that when the dosage of SDS was 0.05 g/L, the highest V leaching rate of 30.1% was obtained. The leaching efficiencies of the metals decreased when the surfactant concentration was adequate. This could be caused by the bacteria growth becoming inhibited under the higher surfactant concentrations [29]. The effect of the surfactants on the

bioleaching of sulfide minerals has been previously investigated, indicating that the addition of surfactants reduces the interfacial tension between the mine and the solution. This is beneficial to the contact of bacteria and mineral contact, which improves the bioleaching [30].

3.5.3 Roasting

The experiment used blank roasting as a pretreatment process in order to improve the conversion rate of vanadium, to reduce the Cl_2, HCl and other harmful gas produced by traditional vanadium extraction. The result of the blank roasting pretreatment test is shown in Fig. 14. The V leaching rate increased in the prophase and the rate of growth stabilized during the late stage. The V leaching rate of *B. mucilaginosus* BM-50 reached 68.3% after 20 days of bioleaching, which was much higher than that of the blank control (18.2%).

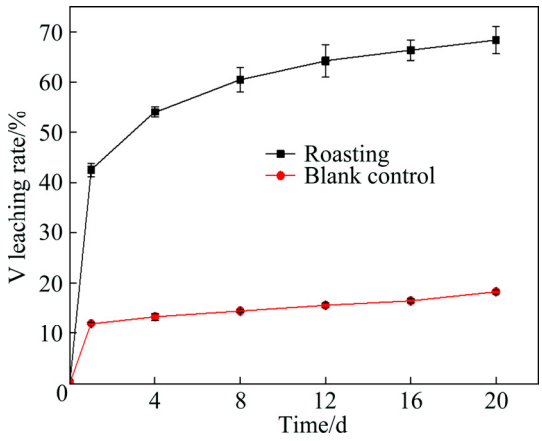

Fig. 14 V leaching rate of leaching system of stone coal pre-processed by roasting

The essence of roasting was the conversion of vanadium-bearing mica to feldspar because vanadium typically exists in the mica [31]. The crystalline structures of mica and feldspar showed that the phase transition between mica to feldspar belonged to the bond-breaking reconstruction. Most of hydroxy in the crystal lattice of the aluminosilicate minerals was removed during the transformation. The vanadium was liberated from the mica [32]. Most of the vanadium in the stone coal occurred with V^{3+}/V^{4+}. The blank roasting pretreatment oxidized the low-valence vanadium into high-priced vanadium, which was beneficial to the leaching of vanadium via bacteria [33].

4 Conclusions

(1) Bacteria were mutated effectively using atmospheric and room temperature plasma mutation. Under a treatment time of 50 s, the total content of the organic acid in the mutagenic strain medium was 162.6 mg/L after 2 days of cultivating, nearly double that of the original strain. The V leaching rate of the mutant was 18.2% after 20 days of leaching.

(2) The SEM−EDS results showed that the mineral particles were corroded by bacteria and the V element gradually dissolved after interactions with bacteria. The FTIR analysis showed that the Si—O—M bending vibration peak at 516 cm^{-1} disappeared, which indicated that the metal ions were dissolved and the basic elements of mica in the stone coal were distorted and collapsed after bacterial leaching.

(3) The results of the enhanced treatments showed that the blank roasting pretreatment had the best effect on the vanadium extraction, which reached 68.3% after 20 days of leaching.

References

[1] ZHAO Yun-liang, WANG Wei, ZHANG Yi-min, SONG Shao-xian, BAO Shen-xu. In-situ investigation on mineral phase transition during roasting of vanadium-bearing stone coal [J]. Advanced Powder Technology, 2017, 28: 1103−1107.

[2] ZHAO Yun-liang, ZHANG Yi-min, BAO Shen-xu, LIU Tao, BIAN Ying, JIANG Mou-feng, LIU Xiang. Loose-stratification model in separation process for vanadium pre-concentration from Stone coal [J]. Transactions of Nonferrous Metals Society of China, 2014, 24: 528−535.

[3] LI Min-ting, WEI Chang, FAN Gang, LI Cun-xiong, DENG Zhi-gan, LI Xin-bin. Pressure acid leaching of black shale for extraction of vanadium [J]. Transactions of Nonferrous Metals Society of China, 2010, 20(S): s112−s117.

[4] LIU Chun, ZHANG Yi-min, BAO Shen-xu. Vanadium recovery from stone coal through roasting and flotation [J]. Transactions of Nonferrous Metals Society of China, 2017, 27: 197−203.

[5] YANG Hong-ying, LIU Qian, CHEN Guo-bao, TONG Lin-lin, ALI A. Bio-dissolution of pyrite by *Phanerochaete chrysosporium* [J]. Transactions of Nonferrous Metals Society of China, 2018, 28: 766−774.

[6] BEHERA S K, PANDA P P, SINGH S, PRADHAN N, SUKLA L B, MISHRA B K. Study on reaction mechanism of bioleaching of nickel and cobalt from lateritic chromite overburdens [J]. International Biodeterioration & Biodegradation, 2011, 65: 1035−1042.

[7] ABDOLLAHI H, NOAPARAST M, SHAFAEI S Z, MANANFI Z, MUNOZ J A, TUOVINEN O H. Silver-catalyzed bioleaching of copper, molybdenum and rhenium from a chalcopyrite–molybdenite concentrate [J]. International Biodeterioration & Biodegradation, 2015, 104: 194−200.

[8] DENG R. Characteristics and mechanisms of vanadium leaching using single and mixed *Acidithiobacillus Ferrooxidans* [D]. Xiangtan: Xiangtan University, 2015. (in Chinese)

[9] WANG Fei, ZHANG Yi-min, LIU Tao, HUANG Jing, ZHAO Jie, ZHANG Guo-bin, LIU Juan. Comparison of direct acid leaching process and blank roasting acid leaching process in extracting vanadium from stone coal [J]. International Journal of Mineral Processing, 2014, 128: 40−47. (in Chinese)

[10] DOPSON M, LOVGREN L, BOSTROM D. Silicate mineral dissolution in the presence of acidophilic microorganisms: Implications for heap bioleaching [J]. Hydrometallurgy, 2009, 96: 288−293.

[11] YANG Xiao-xue, LI Yan, LU An-huai, WANG Hao-ran, ZHU Yun, DIING Hong-rui, WANG Xin. Effect of *Bacillus mucilaginosus* D4B1 on the structure and soil-conservation-related properties of montmorillonite [J]. Applied Clay Science, 2016, 119: 141−145.

[12] STYRIAKOVA I, MOCKOVCIAKOVA A, STYRIAK I, KRAUS I, UHLIK P, MADEJOVA J, OROLINOVA Z. Bioleaching of clays and iron oxide coatings from quartz sands [J]. Applied Clay Science, 2012, 61: 1−7.
[13] ZHAO Jiang-man, WU Wei-jin, ZHANG Xu, ZHU Ming-long, TAN Wen-song. Characteristics of bio-desilication and bio-flotation of *Paenibacillus mucilaginosus* BM-4 on aluminosilicate minerals [J]. International Journal of Mineral Processing, 2017, 168: 40−47.
[14] FANG Ming-yue, JIN Li-hua, ZHANG Chong, TAN Yin-ye, JIANG Pei-xia, GE Nan, LI He-ping, XING Xin-hui. Rapid mutation of *Spirulina platensis* by a new mutagenesis system of atmospheric and room temperature plasmas (ARTP) and generation of a mutant library with diverse phenotypes [J]. Plos One, 2013, 8: e77046.
[15] LI Xiang-yu, LIU Rui-jie, LI Jing, CHANG Ming, LIU Yuan-fa, JIN Qing-zhe, WANG Xing-guo. Enhanced arachidonic acid production from *Mortierella alpina* combining atmospheric and room temperature plasma (ARTP) and diethyl sulfate treatments [J]. Bioresource Technology, 2015, 177: 134−140.
[16] LAN Zhuo-yue, HU Yue-hua, QIN Wen-qing. Effect of surfactant OPD on the bioleaching of marmatite [J]. Minerals Engineering, 2009, 22: 10−13.
[17] LIU Wei, YANG Hong-ying, SONG Yan, TOMG Lin-lin. Catalytic effects of activated carbon and surfactants on bioleaching of cobalt ore [J]. Hydrometallurgy, 2015, 152: 69−75.
[18] ZHAO Yun-liang, ZHANG Yi-min, SONG Shao-xian, CHEN Tie-jun, BAO Shen-xu. Behaviors of impurity elements Ca and Fe in vanadium-bearing stone coal during roasting and its control measure [J]. International Journal of Mineral Processing, 2016, 148: 100−104.
[19] LU Yuan, WANG, Li-yan, MA Kun, LI Guo, ZHANG Chong, ZHAO Hong-xin, LAI Qi-heng, LI He-ping, XING Xin-hui. Characteristics of hydrogen production of an *Enterobacter aerogenes* mutant generated by a new atmospheric and room temperature plasma (ARTP) [J]. Biochemical Engineering Journal, 2011, 55: 17−22.
[20] CAO Song, ZHOU Xu, JIN Wen-biao, WANG Feng, TU Ren-jie, HAN Song-fang, CHEN Hong-yi, CHEN Chuan, XIE Guo-Jun, MA Fang. Improving of lipid productivity of the oleaginous microalgae *Chlorella pyrenoidosa* via atmospheric and room temperature plasma (ARTP) [J]. Bioresource Technology, 2017, 244: 1400−1406.
[21] LEE Y, KIM K, KANG K T, LEE J S, YANG S S, CHUNG W H. Atmospheric-pressure plasma jet induces DNA double-strand breaks that require a Rad51-mediated homologous recombination for repair in *Saccharomyces cerevisiae* [J]. Archives of Biochemistry and Biophysics, 2014, 560: 1−9.
[22] ZHU Yun, LI Yan, LU An-huai, WANG Hao-ran, YANG Xiao-xue, WANG Chang-qiu, CAO Wei-zheng, WANG Qing-hua, ZHANG Xiao-lei, PAN Dan-mei, PAN Xiao-hong. Study of the interaction between bentonite and a strain of *bacillus* [J]. Clays and Clay Minerals, 2011, 59: 538−545.
[23] ZHAO Jiang-man, WU Wei-jin, ZHANG Xu, ZHU Ming-long, TAN Wen-song. Characteristics of bio-desilication and bio-flotation of *Paenibacillus mucilaginosus* BM-4 on aluminosilicate minerals [J]. International Journal of Mineral Processing, 2017, 168: 40−47.
[24] XIAO Guo-guang, SUN De-si, CAO Fei. Weathering of silicate minerals by metabolites produced by silicate bacteria in culture experiments [J]. Journal of Mineralogy and Petrology, 2013, 33: 8−15. (in Chinese)
[25] ZHANG Xian-zhen, LIN Hai, SUN De-si, ZHANG Min. Structural effects of sillicate minerals on the growth, metabolism and desilicification of a strain of silicate bacterium [J]. Journal of Chongqing University, 2014, 37: 98−103. (in Chinese)
[26] WENG Shi-fu. Fourier transform infrared spectroscopy [M]. 2nd ed. Beijing: Chemical Industry Press, 2010. (in Chinese)
[27] ZHU Yun, CAO Wei-zheng, LU An-huai, WANG Qing-hua, LI Yan, ZHANG Xiao-lei, WANG Chang-qiu. A study of the interaction between montmorillonite and a strain of *Bacillus mucilaginosus* [J]. Acta Petrologica et Mineralogica, 2011, 30: 121−126.
[28] LIU Juan, ZHANG Yi-min, HUANG Jing, LIU Tao, YUAN Yi-zhong, HUANG Xian-bao. Influence of mechanical activation on mineral properties and process of acid leaching from stone coal [J]. Chinese Journal of Rare Metals, 2014, 38: 115−122. (in Chinese)
[29] LIU Wei, YANG Hong-ying, SONG Yan, TONG Lin-lin. Catalytic effects of activated carbon and surfactants on bioleaching of cobalt ore [J]. Hydrometallurgy, 2015, 152: 69−75.
[30] PENG An-an, LIU Hong-chang, NIE Zhen-yuan, XIA Jin-lan. Effect of surfactant Tween-80 on sulfur oxidation and expression of sulfur metabolism relevant genes of *Acidithiobacillus ferrooxidans* [J]. Transactions of Nonferrous Metals Society of China, 2012, 22: 3147−3155.
[31] ZHAO Yun-liang, WANG Wei, ZHANG Yi-min, SONG Shao-xian, BAO Shen-xu. In-situ investigation on mineral phase transition during roasting of vanadium-bearing stone coal [J]. Advanced Powder Technology, 2017, 28: 1103−1107.
[32] JIANG Mo-feng. Study on mechanism of extracting vanadium by blank roasting and acid leaching from mica-type stone coal [D]. Wuhan: University of Technology Wuhan, 2015.
[33] LI Long-tao, ZHU Pei-wang, ZHENG lun-shi, JIANG Xiao, ZENG Wei-qiang. Additive-free roasting technique for extracting vanadium from residue of mica-type vanadium-bearing stone coal [J]. Chinese Journal of Rare Metals, 2014, 38: 480−486.

等离子体诱变菌浸出及石煤的空白焙烧相结合提高石煤中钒浸出效果

董颖博[1,2]，刘 悦[1]，林 海[1,2]，刘陈静[1]

1. 北京科技大学 能源与环境工程学院，北京 100083；
2. 工业典型污染物资源化处理北京市重点实验室，北京 100083

摘 要：为了提高石煤中钒的浸出效率，采用空白焙烧及微生物浸出相结合的方法，以胶质芽孢杆菌为原始菌，采用等离子体技术对其进行诱变处理。结果表明，培养 2 天后，照射时间为 50 s 时所得诱变菌 *B. mucilaginosus* BM-50 代谢产生的总有机酸含量较原始菌株提高近 1 倍。含钒石煤浸出 20 天时，诱变菌 *B. mucilaginosus* BM-50 的钒浸出率达到 18.2%，相比原始菌的钒浸出率(15.3%)有所提高。空白焙烧预处理可以进一步提高钒浸出效率，浸出 20 天时，诱变菌 *B. mucilaginosus* BM-50 的钒浸出率为 68.3%，较未预处理的诱变菌浸出体系的钒浸出率大大提高。研究表明，采用等离子体诱变菌浸出与空白焙烧相结合的方法具有提高低品位石煤钒回收率的巨大潜力。

关键词：常温常压等离子体(ARTP)；胶质芽孢杆菌；含钒石煤；空白焙烧；生物浸出

(Edited by Bing YANG)